Dynamics of Linear Poly(methylphenylsiloxane) by Time-Resolved Fluorescence: Slow vs Fast Relaxations and Low-Temperature Behavior in Chains of Different Lengths

Fernando B. Dias,[*,†] **João C. Lima,**[⊥] **Arturo Horta,**[‡] **Inés F. Piérola,**[‡] **and Antonio L. Maçanita**[†,§]

Instituto de Tecnologia Química e Biológica (ITQB), Oeiras, Portugal; Department Fisicoquímica (CTFQ), Universidad a Distancia (UNED), Madrid, Spain; and Instituto Superior Técnico (IST/UTL), Lisboa, Portugal
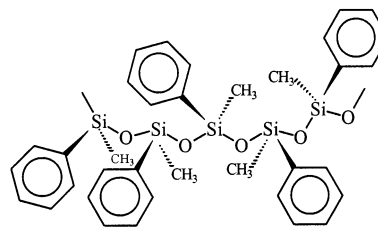
ABSTRACT: Three linear poly(methylphenylsiloxane) chains (PMPS*N*) with different number of skeletal bonds ($N = 82, 284, 1285$) were studied by time-resolved fluorescence spectroscopy in the temperature range 20 to −60 °C. Fluorescence decays obtained for all the samples could be fitted only with sums of three exponential functions. Two different time regimes of excimer formation are detected in these polymers (the same as was previously obtained for a shorter oligomer, PMPS25). A fast relaxation, which is connected to unrestricted skeletal motions at the dyad level, and a slower relaxation, which is attributed to segmental chain rearrangements needed to release temporary isolated hindered monomers. The rate constants of the fast relaxation ($k_a = 14-17$ ns^{-1}, at 20 °C) are one order of magnitude larger than the rate constants of the slower relaxation ($k_u = 1.2-1.6$ ns^{-1}, at 20 °C), and the activation energies of this slow relaxation (E_u) are about 3 kcal mol^{-1} larger than the activation energies of the fast relaxation ($E_a = 2.0-2.2$ kcal mol^{-1}). These rate constants and activation energies are practically constant in all samples, which means that internal dynamics (local or segmental) is not affected by chain length. The fraction of temporary isolated hindered monomers at 20 °C ($\beta = 0.03$) is also constant for all chain lengths, but its low-temperature behavior is systematically dependent on chain length. With decreasing temperature, β first decreases and then increases, the temperature for this trend reversal being higher the longer the chain. At still lower temperatures aggregation takes place, and this is also dependent on chain length.

Introduction

Polymers with chromophores inserted in their repeat units offer an excellent way to probe the internal polymer dynamics in the very fast time regime. Indeed, the fluorescence emission of those chromophores can be directly affected by dynamic[1−3] and conformational chain properties.[4−6] After the absorption of one photon, the excited chromophore can remain more or less temporary isolated or interact with another chromophore. In the first case, the excited monomer decays to the ground state with its lifetime, but in the second case, the monomer emission will be quenched by excimer formation after some segmental chain motions needed to bring the two monomers together. If the chain relaxation times are shorter than or similar to in magnitude the monomer lifetime, the rate constants and the respective energy barriers involved in the internal polymer dynamics can be probed by following the excimer formation kinetics with the appropriate time resolution.

A priori, this is a very simple concept, but in practice it turns out to be complex due to the fact that polymer fluorescence decays are generally multiexponential and difficult to be interpreted.[7−10] Frequently pointed as reasons for that complexity are (1) intramolecular energy transfer or even energy migration,[11−14] (2) more

Chart 1. Linear PMPS*N* Chain

than one class of excimers,[15−17] and (3) the existence of kinetically different monomers.[9,18−20]

In this work, three linear poly(methylphenylsiloxane) chains (PMPS*N*; see Chart 1) with nominal number of skeletal bonds, *N*, equal to 82, 284, and 1285 were studied using picosecond time resolution. In a previous study we presented similar results for a shorter chain ($N = 25$),[32] and adding the present results, we have now a range of chain lengths, extending from oligomer to high polymer, for a discussion of molecular weight dependence. The influence of molecular weight on the fluorescence of polymers showing excimer emission has been studied in a number of systems.[21−31] Most of these studies refer just to stationary data (the excimer to monomer intensity ratio), and only very few report on decays as a function of molecular weight. Thus, the influence of chain length on kinetic data is still lacking, in general.

The chains studied here have a phenyl ring in each repeat unit, so that excimer formation occurs between nearest neighbors. This is a local process, and it can be argued that the dynamics of such a process should not change much with chain length. But the results with
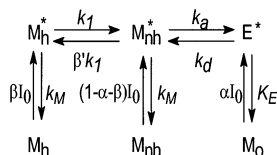
Scheme 1. Kinetic Mechanism

$$M_h^* \underset{\beta' k_1}{\overset{k_1}{\rightleftarrows}} M_{nh}^* \underset{k_d}{\overset{k_a}{\rightleftarrows}} E^*$$

$$\beta I_0 \Big\updownarrow k_M \quad (1-\alpha-\beta)I_0 \Big\updownarrow k_M \quad \alpha I_0 \Big\updownarrow K_E$$

$$M_h \qquad\qquad M_{nh} \qquad\qquad M_0$$

the oligomer PMPS25 have shown that excimer formation occur in two different time regimes. One is associated with the unrestricted approaching motions controlled just by local bond rotations at the level of a single dyad; the other is associated with a ten-fold slower transition caused by retarded motions in which the local bond rotations occur only after a delay time caused by the coupling of the dyad to the attached chain. The fast unrestricted local motion at the dyad level is expected to be little affected by chain length, but the retarded motion in which the coupling to the chain imposes a delay can be more dependent on chain length. Here, we have an adequate set of samples to analyze this possibility.

The distinction between a fast dyad-like motion and a retarded motion delayed by the chain has been based on the following three findings. First,[32] the chain PMPS25 has in common with the dyad model molecule PMPS2 a short and a long decay times (order of 0.1 and 10 ns, respectively). An intermediate decay time is found in the chain PMPS25 but not in the dyad model molecule PMPS2. Second,[33] this intermediate decay time appears also in the cyclic trisiloxane where one of the phenyl rings is permanently isolated or hindered because of configuration (the trans phenyl ring). The contribution of this intermediate component to the decays is in accordance with the fraction of phenyl rings which are in trans configuration in the cyclic trisiloxane. Third,[32,34] in molecular dynamics simulations (MD) for the interphenyl distance variation as a function of time (carried out for a simple dyad and for polymer fragments containing 14 and 28 skeletal bonds), only one time regime of phenyl approach was found for the simple dyad, but for dyads inside a polymer chain, two time regimes of monomer approach were detected: a dyad-like fast transition and a much slower transition where one chromophore remains away of their two consecutive neighbors during certain time lags. In the linear chains there is no ring closure which isolates a given configuration, but the monomers get temporarily trapped or "frozen" in conformations which are non-excimer-forming; hence, a slow relaxation is also possible in them (in fact, the intermediate decay was observed for PMPS25).

The two relaxations can be associated with the classification of monomers in two categories: one, called unrestricted or nonhindered monomers (M_{nh}), and the other called temporary isolated or hindered monomers (M_h). In the decays, the nonhindered monomers give rise to the fast component, and the hindered monomers give rise to the slow component. In fact, the decays of PMPS25 were triexponential, and a kinetic scheme including three excited-state species (M_{nh}, M_h, and the excimer E) was needed to adequately interpret the results.[32] The same kinetic scheme (Scheme 1) will be used here for the other chain lengths. Of the three new chain lengths considered now, we shall use a full kinetic analysis for the short ($N = 82$) and the long ($N = 1285$) ones and a simplified analysis for the intermediate chain ($N = 284$).

In this range of chain lengths some differences in behavior had been detected at low temperatures. By ^{1}H NMR and steady-state fluorescence, it was detected that the long chains (N from 176 to 1285) suffer a drastic reduction of the segment mobility at temperatures below ca. -50 °C. This phenomenon was also accompanied by the increase of light scatter intensity and by the decrease of excimer stability, suggesting that a phase transition occurs below that temperature.[35] These facts were not seen with short chains ($N = 25$ and $N = 82$), meaning that a minimum chain length is necessary to observe that transition. Therefore, it seems of interest to extend the study in this range of chain lengths to the kinetic behavior detected by picosecond time-resolved fluorescence. In summary, we wanted to know whether the two relaxation processes detected in the short oligomer (PMPS25) are also present in longer chains and whether those processes can be connected with the transition at low temperatures (segment mobility loss) that was detected only for the long chains.[35]

Experimental Section

Atactic poly(methylphenylsiloxane) samples, synthesized and characterized by S. J. Clarson and J. A. Semlyen in Prof. Semlyen's laboratory,[36] were represented by PMPSN (N being the nominal number-average number of skeletal bonds). PMPSN molecular weights and polydispersities were as described before:[35] $M_n \times 10^{-3}$ (M_w/M_n) = 1.89 (1.06); 5.73 (1.05); 19.51 (1.12); 93.0 (2.00), for $N = 25$; 82; 284; 1285, respectively.
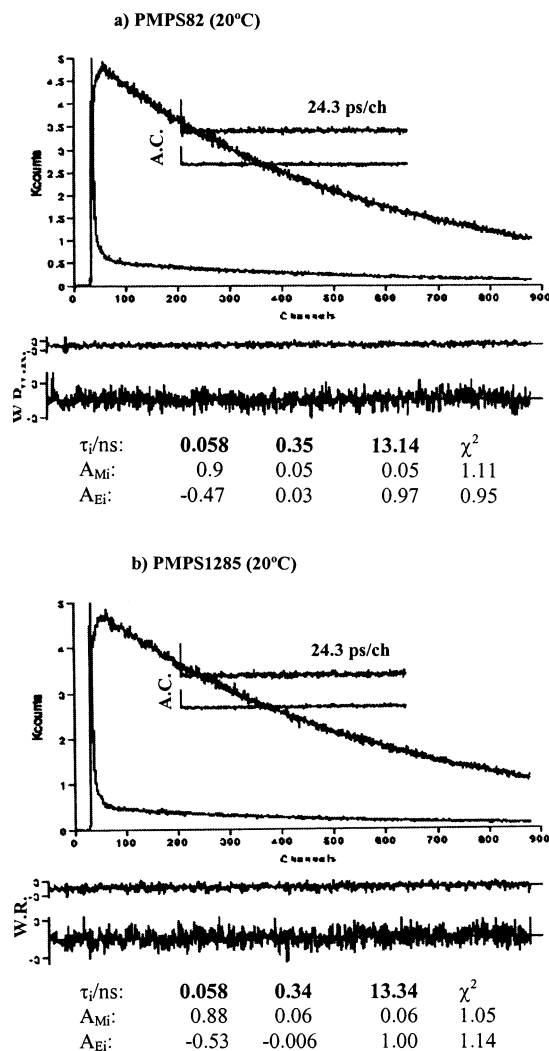
Methylcyclohexane (MCH) was purchased from BDH and purified as previously described.[37] Solutions of absorbance less than 0.5 at the excitation wavelength (260 nm) were degassed by the freeze−pump−thaw technique (six cycles at 10^{-4} Torr) and then sealed. Polymer concentrations, given in moles of chromophore unit per liter, were in the range 2×10^{-4}−4×10^{-3}, which is below the critical value for coil overlap. Moreover, the low absorbance of the samples prevents self-absorption or the inner filter effect.

Ultraviolet absorption and fluorescence spectra were recorded on an Olis-15 spectrophotometer and a SPEX Fluorolog 2 fluorimeter, respectively. Light scattering was measured on the fluorescence spectra at an incident radiation of $\lambda = 350$ nm, a wavelength at which the samples do not absorb.

Fluorescence decays were measured using picosecond time-correlated single photon counting (TCSPC), as described before.[2,37] A frequency-tripled Ti:sapphire picosecond laser system (Spectra Physics Inc.), pumped by a Ar$^+$ or a Millenia X, both from Spectra Physics Inc., was the excitation source ($\lambda_{ex} = 260$ nm, repetition rate 4 MHz, fwhm = 28 ps). Temperature control was achived using a homemade system based on cooled nitrogen and electric heating, which is automatically controlled by the difference between the input temperature value and the sample real temperature, determined with a PT100 thermometer. Alternate collection of pulse and sample was performed (10^3 counts at the maximum per cycle) until 5×10^3 counts at the maximum were acquired. The fluorescence decays were deconvoluted in a PC (Pentium III, 128 Mb RAM), using the Linux version of the George Striker's program.[38]

Results and Discussion

Decays. Fluorescence decays for all samples were collected at both monomer and excimer wavelengths of respectively 275 and 330 nm. Figure 1 shows global analysis of PMPS82 and PMPS1285 fluorescence decays at 20 °C. Perfect fits were obtained only with sums of three exponential functions. Decay times (τ_i) and experimental amplitudes (A_{Mi} and A_{Ei}) are very similar on both monomer and excimer decays and are also

a) PMPS82 (20°C)

24.3 ps/ch

τ_i/ns:	**0.058**	**0.35**	**13.14**	χ^2
A_{Mi}:	0.9	0.05	0.05	1.11
A_{Ei}:	-0.47	0.03	0.97	0.95

b) PMPS1285 (20°C)

24.3 ps/ch

τ_i/ns:	**0.058**	**0.34**	**13.34**	χ^2
A_{Mi}:	0.88	0.06	0.06	1.05
A_{Ei}:	-0.53	-0.006	1.00	1.14

Figure 1. Fluorescence decays of PMPS82 (a) and PMPS1285 (b) collected at the monomer and excimer wavelengths, in MCH at 20 °C, and results from global analysis: autocorrelation function A.C.; weighted residuals W.R.; and χ^2 values. τ_i, decay times; A_{Mi} and A_{Ei}, amplitudes of (respectively) monomer and excimer.

similar to the values obtained for PMPS25.[32] Results obtained for PMPS284 show that also in this sample sums of three exponential functions are needed to fit the fluorescence decays. Hence, the exception to this triple-exponential behavior is just the dyad model molecule PMPS2. For this small model molecule two exponential functions are sufficient to fit the excited state fluorescence decays. In PMPS2 the dyad is free, not inserted inside a longer chain; hence, the monomers are nonhindered, and only the fast process is expected, which in the decays translates into the absence of a third exponential.[32]

Table 1 summarizes the experimental data obtained at 20 °C from the simultaneous analysis of monomer and excimer fluorescence decays (global analysis), for PMPS82, PMPS284, and PMPS1285 (PMPS25 is also presented for comparison).

Figure 2 shows the temperature dependence of the decay parameters (decay times τ_i and amplitudes A_{Mi} and A_{Ei}) for PMPS25,[32] PMPS82, and PMPS1285. Data for PMPS82 and PMPS1285 were obtained at temperatures above −60 and −20 °C, respectively, due to contamination of the decays with scattered light below those temperatures.

Table 1. Summary of Decay Times and Amplitudes from Global Analysis of Several PMPSN Samples (N = 25, 82, 284, 1285) in MCH at 20 °C

compound		τ_3 (ns)	τ_2 (ns)	τ_1 (ns)	χ^2
PMPS25					
		0.064	0.38	13.14	
	A_{Mi}:	0.92	0.05	0.03	1.03
	A_{Ei}:	−0.54	−0.02	1.00	0.95
PMPS82					
		0.058	0.35	13.14	
	A_{Mi}:	0.90	0.05	0.05	1.11
	A_{Ei}:	−0.47	0.03	0.97	0.95
PMPS284					
		0.06	0.38	13.21	
	A_{Mi}:	0.94	0.03	0.03	0.95
	A_{Ei}:	−0.56	0.02	0.98	0.99
PMPS1285					
		0.058	0.34	13.34	
	A_{Mi}:	0.88	0.06	0.06	1.05
	A_{Ei}:	−0.53	−0.006	1.00	1.14

Kinetic Model and Data Analysis. Scheme 1 shows the proposed kinetic mechanism of excimer formation in PMPSN chains. This mechanism predicts triple-exponential fluorescence decays for monomer and excimer, which is in agreement with experimental observation. It was first developed to explain the excimer formation process in PMPS25.[32]

The mechanism considers two modes of excimer formation involving three excited-state species. These are nonhindered monomers (M_{nh}), temporary isolated hindered monomers (M_h), kinetically coupled with nonhindered monomers, and excimers (E) (see Scheme 1). The rate constant of the fast excimer formation between nonisolated monomers (M_{nh}) is represented by k_a, the rate constant of excimer reversibility is represented by k_d, and the rate constants of excimer and monomer decays are represented by k_E and k_M, respectively. The rate constant of the slower relaxation is k_1, and β represents the fraction of temporary isolated hindered monomers. The parameter β' in Scheme 1 represents the equilibrium constant between temporary isolated hindered monomers (β) and nonisolated monomers ($1 - \beta$):

$$\beta' = \frac{\beta}{1 - \beta} \tag{1}$$

The model also takes into account the direct absorption of light by a fraction of monomer units, α, which are in preformed ground-sate dimer states.

The analysis of decays based on this kinetic scheme has been described in detail before.[32] We have seven kinetic parameters (k_a, k_d, k_1, k_E, k_M, β, α) to be determined from the decay times and amplitudes of Figure 2. Because this full analysis of time-correlated data is slow and complex, we tried also a simplified approximate method to obtain the rate constant of excimer formation (k_a) and the respective energy activation (E_a) for one of the samples: PMPS284. The approximate value of k_a is obtained from τ_3, the fastest component observed in the decays, and k_M, the lifetime of the monomeric model compound (MS),[39] as

$$k_a = \frac{1}{\tau_3} - k_M \tag{2}$$

In Figure 3, excimer formation rate constants k_a obtained from the complete kinetic model solution and from the approximate eq 2 for PMPS25 are compared.
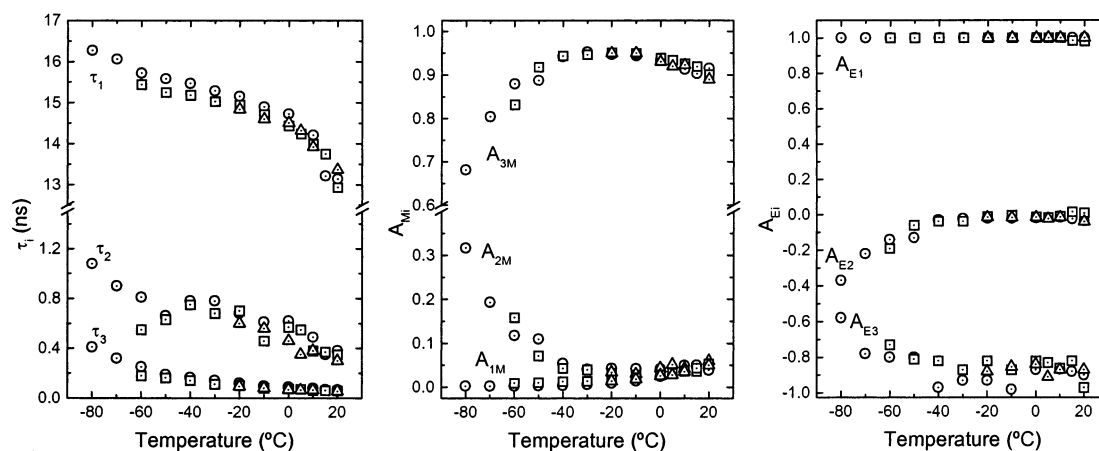
Figure 2. Temperature dependence of the decay parameters (decay times, τ_i, and amplitudes, A_{Mi} and A_{Ei}) for PMPS25[32] (○), PMPS82 (□), and PMPS1285 (△).
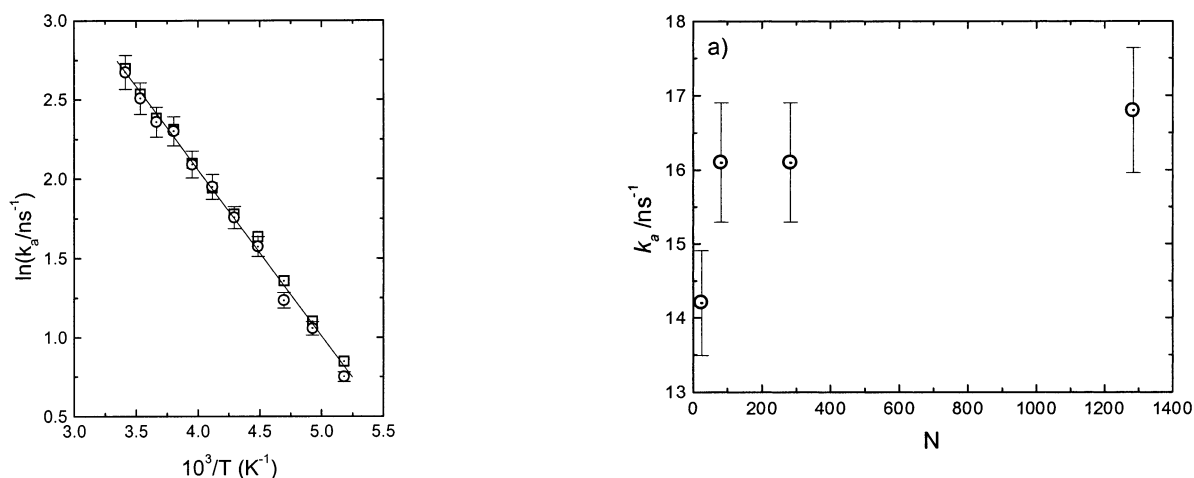

Figure 3. Arrhenius type plot of k_a for PMPS25 obtained from the complete kinetic model solution (○) and from eq 2 (□).

Observed differences are within the experimental error, which confirms the possibility of obtaining k_a and E_a for PMPS284 with good accuracy with this simplified approximate method.

Chain Length Dependence. In most of the temperature range considered, the decay times and experimental amplitudes have similar values for the three samples, which points to an excimer formation process globally independent of the chain length (see Figure 2).

Figure 4 shows the rate constant of the fast excimer formation process, k_a, at 20 °C and the respective activation energy, E_a, as functions of chain length. The rate constant k_a shows an increase from 14.2 ns^{-1} in PMPS25 to 16.1 ns^{-1} for PMPS82, but for longer chains the value remains constant within the experimental error. This fact suggests a fast excimer formation process slightly more effective in the long chains, but reaching an asymptotic limit fairly soon. This type of variation of the rate constant of excimer formation with molecular weight has been also observed in the case of polystyrene chains.[40]

The activation energy E_a is practically constant for all chain lengths. Therefore, we must admit that chain length does not affect the internal dynamics of nonhindered monomers in PMPSN linear chains in the temperature range considered. These chain local motions are affected neither by global chain properties nor by conformational restrictions as occurs in the cycles.[32,33]
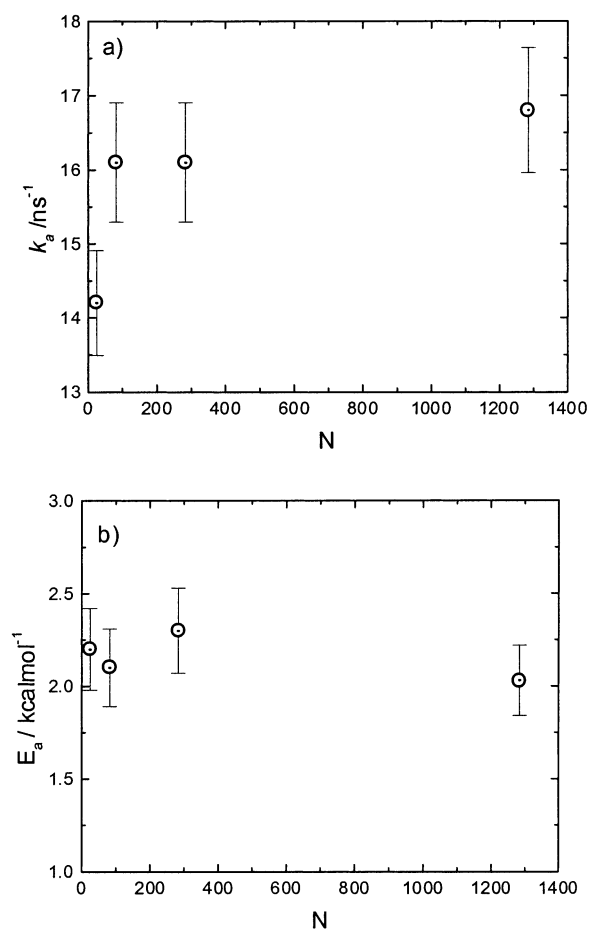
Figure 4. Rate constant of excimer formation k_a at 20 °C (a) and the respective activation energy E_a (b) as a function of chain length.

The other kinetic parameters obtained from the full analysis of decays for PMPS82 and PMPS1285 are shown in Figure 5 (data for PMPS25 also included for comparison). Figure 5a shows the Arrhenius type plots for the rate constants k_i, and Figure 5b shows the temperature dependence of the fraction of temporary hindered monomers (β). Table 2 contains additional relevant data. We can see that similar values for all the kinetic parameters and their temperature variation are obtained for the three samples. This means that chain length does not significantly affect the general features of the polymer internal dynamics.
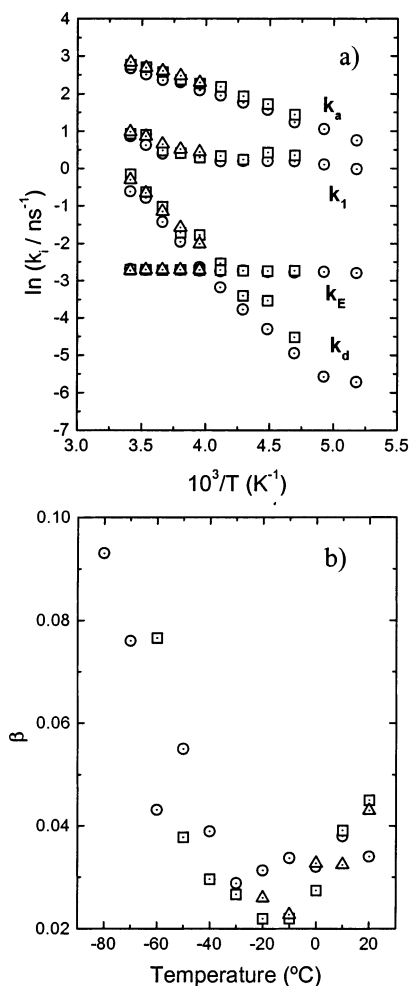
Figure 5. Temperature dependence of the rate constants k_i and the fraction of temporary isolated hindered monomers (β) for PMPS82 ($\square$) and PMPS1285 ($\triangle$) in MCH solution. Data from PMPS25[32] ($\bigcirc$) also included.

Table 2. Values of Rate Constants, Activation Energies, and Fractions of Temporary Hindered Monomers (β) and Preformed Dimers (α) Obtained for PMPS25, PMPS82, and PMPS1285, in MCH Solution, from Time-Resolved Results

	PMPS25	PMPS82	PMPS1285
$k_a^{20°C}/10^9 \text{ s}^{-1}$	14.2 ± 0.5	16.1 ± 0.8	16.8 ± 0.6
$k_d^{20°C}/10^9 \text{ s}^{-1}$	0.58 ± 0.1	0.86 ± 0.2	0.74 ± 0.2
$k_u^{20°C}/10^9 \text{ s}^{-1}$	1.21 ± 0.2	1.23 ± 0.2	1.55 ± 0.3
$k_t /10^9 \text{ s}^{-1}$	0.58 ± 0.1	0.58 ± 0.15	0.58 ± 0.3
$k_M^{20°C}/10^9 \text{ s}^{-1}$	0.267 ± 0.003	0.267 ± 0.003	0.267 ± 0.003
$k_E^{20°C}/10^9 \text{ s}^{-1}$	0.068 ± 0.006	0.066 ± 0.007	0.067 ± 0.006
E_a/kcal mol^{-1}	2.2 ± 0.2	2.01 ± 0.2	2.03 ± 0.2
E_d/kcal mol^{-1}	6.9 ± 0.3	6.6 ± 0.4	6.4 ± 0.3
E_u/kcal mol^{-1}	4.73 ± 0.5	5.09 ± 0.51	5.3 ± 0.53
$\alpha^{20\,°C}$	0.05 ± 0.02	0.07 ± 0.03	0.08 ± 0.02
$\beta^{20\,°C}$	0.04 ± 0.02	0.03 ± 0.02	0.03 ± 0.02

Not only the fast excimer formation, k_a, but also the slow conversion of hindered monomers into nonhindered monomers, k_1, is practically the same in all chain lengths. This k_1 contains the cooperative segmental rearrangements required for the release of temporary hindered monomers (see below). Its constancy with chain length means that this segmental rearrangements are also somehow local processes not affected by global chain properties. However, in this case the site involved should extend over a certain chain fragment and not just a simple dyad. The same practical constancy with chain length can be seen in the fraction of ground-state

preformed dimers, α, and in the fraction of temporary isolated hindered monomers, β. In the dyad model molecule, PMPS2, there was no contribution from preformed ground-state dimers and also temporary hindered monomers do not exist.[32] The nonvanishing values of α and β in the polymer samples reflect that these contributions arise because chromophores are inside a chain and not in a free dyad. But their constancy with chain length means that just a segment or fragment of the chain is enough, and there is no influence of the global properties of the chain.

The Slow Relaxation. We have called as temporary isolated or hindered, M_h, those monomers that are temporary frozen in "conformations" where no excimer can occur during a given time. Such frozen "conformations" are the result of some kinetic restraint imposed on the monomer by the rest of the chain (at least a rather long fragment should be needed for this kinetic restraint because of the intrinsic flexibility of the siloxane backbone). The formation of excimer gets then delayed until the monomer is released from such "conformation" by an adequate rearrangement of the chain, possibly, a cooperative motion of chain segments. These cooperative rearrangements occur with a rate constant k_u. When the temporary hindered monomer (M_h) is released, it converts into a nonhindered monomer (M_{nh}), which is able to undergo excimer formation by the fast dyad-like process. Thus, the rate k_1, which represents the conversion of M_h into M_{nh}, contains this k_u of chain (cooperative) rearrangement. But the conversion of M_h into M_{nh} can occur also without chain rearrangement, simply by energy transfer from the temporary hindered monomer to a neighboring nonhindered monomer.[33] Let us call k_t the rate constant for such energy transfer. The global rate constant of the slower relaxation (k_1) is then the sum of the rate constant associated with the cooperative chain motions (k_u) and the rate constant of energy transfer between one temporary isolated hindered monomer and their two nearest neighbors (k_t) times the probability that these are not isolated monomers ($1 - \beta$):

$$k_1 = k_u + 2(1 - \beta)k_t \qquad (3)$$

To evaluate the rate constant due to cooperative chain rearrangement (k_u), the k_1 data of the three polymers were globally fitted to eq 3, with a common k_t value and the assumption of an Arrhenius type form for $k_u = k_u^0 \exp(-E_u/RT)$, where k_u^0 and E_u were the adjustable parameters for each of the three data sets. The results are shown in Figure 6. A summary of all the kinetic parameters determined is given in Table 2.

The value of the slow rate constant at 20 °C ($k_u = 1.21-1.55 \text{ ns}^{-1}$) is one order of magnitude lower than the fast relaxation rate constant ($k_a = 14.2-16.8 \text{ ns}^{-1}$) for all samples. The value of the energy transfer rate constant ($k_t = 0.58 \text{ ns}^{-1}$) is still lower. k_u seems to slightly increase with chain length from 1.21 ns^{-1} for PMPS25 to 1.55 ns^{-1} for PMPS1285, but we have not sufficient precision in this parameter to consider significant that variation. The values of the activation energy for the slow relaxation, E_u, range from 4.7 kcal mol^{-1} in PMPS25 to 5.3 kcal mol^{-1} in PMPS1285, which are much larger than the value of the activation energy for the fast relaxation ($E_a = 2.0-2.2 \text{ kcal mol}^{-1}$) and the value for the energy activation for viscous flow in MCH (2.4 kcal mol^{-1}).[18,19]
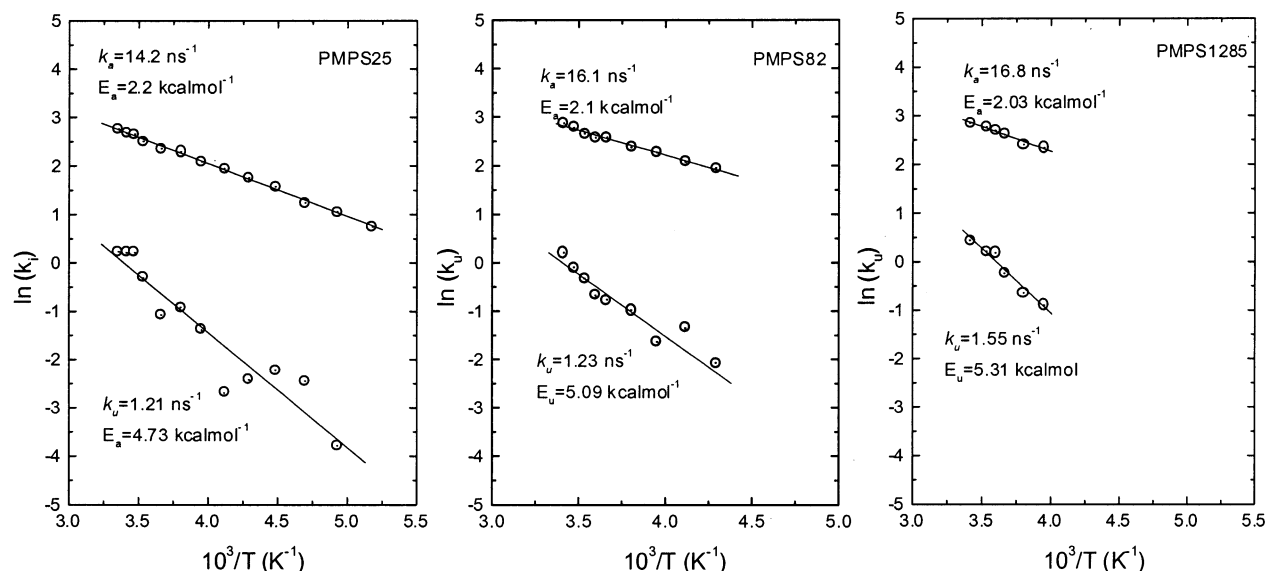
Figure 6. Arrhenius type plot of k_a and k_u for PMPS25, PMPS82, and PMPS1285.

Therefore, the relaxation process involving cooperative segmental motions controlled by chain rearrangements (k_u) is ten-fold slower than the local dyad-like relaxation and is activated by an apparent barrier about 3 kcal mol^{-1} above the activation of the fast process. This additional barrier should be originated in some way by the chain segments which temporary "freeze" the hindered monomers. The siloxane backbone bonds have very low torsional barriers, confering a great conformational flexibility to these polymer chains, so we have to look elsewhere for the origin of the barrier. The value (3 kcal mol^{-1}) is the same as the energy well in the conformational map of a dyad of this polymer.[4] The interaction between phenyl rings of contiguous units in the chain is attractive (for the distances involved). When the two rings of a dyad approach from a conformation in which they are distant to a conformation in which they adopt the sandwich-like pairing required for excimer formation, the conformational energy decreases by 3 kcal mol^{-1}. In a polymer chain several dyads are in a sandwich-like pairing at any given moment. Such conformations are being formed and broken continuously in all the dyads, giving a certain average fraction of dyads in excimer forming conformations. For a temporary isolated monomer to be released, some rearrangement in the distribution of conformations of the other dyads has to occur. On the average, one excimer forming conformation has to be lost by the rest of the chain to release the temporary hindered monomer, and this loss costs 3 kcal mol^{-1} of conformational energy. (The same energy will be recovered when the released monomer goes to an excimer forming conformation, but the process of the released monomer belongs already to the fast type.) Admittedly, this is a very vague speculation on the origin of the high activation energy for the slow relaxation. But if this were really the origin, one would expect this barrier to be even higher in polymers with aromatic rings of a size larger than phenyl, because the interchromophore attraction would be then stronger. If the chain were hydrocarbon instead of siloxane, then the "fast" excimer formation (k_a) would be much slower, of the order of the k_u determined here, and the "slow" relaxation still slower.

Low-Temperature Behavior. Interestingly, the fraction of temporary isolated monomers (β) decreases from room temperature to -30 °C (PMPS25), -20 °C (PMPS82), and -10 °C (PMPS1285), but below this value, β increases on lowering temperature (see Figure 5b). Not only the values of this parameter but also the patterns followed by its temperature variation are similar for all chain lengths. The differences arise only in the temperature value where the up-turn (decrease-to-increase) occurs. This temperature is lower the shorter the chain. At temperatures still lower (below -60 °C for PMPS25 or -40 °C for PMPS1285), the behavior is dominated by an aggregation process of the chain. This is clearly demonstrated by the light scattering results.

Figure 7 shows the light scattering intensity, I_{LS}, at an incident radiation of $\lambda = 350$ nm (a wavelength at which the samples do not absorb), for PMPS25 and PMPS1285, as a function of temperature. I_{LS} intensity decreases for the two samples from 20 to -40 °C for PMPS1285 and to -60 °C for PMPS25, but below those temperatures I_{LS} intensity increases, which can be explained by a gradual contraction of the polymer coil followed by molecular aggregation. The aggregation is not important in the short chain PMPS25, as the increase in light scattering for temperatures below -100 °C simply recovers the same value that it has at room temperature. But, in the case of the long chain PMPS1285, the increase in scattered light intensity is 50-fold, which points to a high aggregation number in this case. This aggregation is more important in the longer chain as expected, because polymer solubility decreases with increasing chain length. (However, solubility is no problem for the preparation of the samples at room temperature, since this polymer has a Mark–Houwink exponent for the intrinsic viscosity which, in the present solvent (MCH) at 20 °C, is $a = 0.58$,[41] well above the critical value 0.5 for Θ solvents.)

Conclusions

In the internal dynamics leading to excimer formation in linear PMPS*N* samples, some monomers are temporary isolated or hindered. Although the fraction of these temporary hindered monomers is small, it is consistently found in all samples and has the same value for all chain lengths.
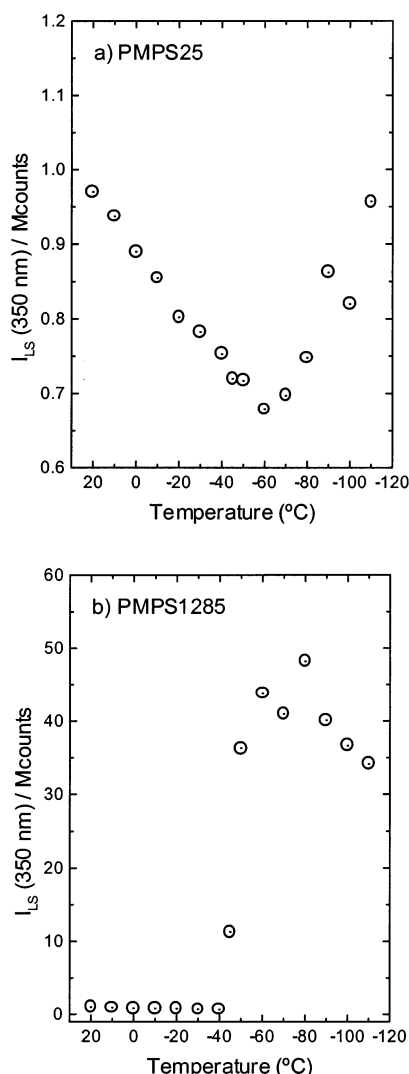
Figure 7. Light scattering intensity, I_{LS}, at an incident radiation of $\lambda = 350$ nm (a wavelength at which the samples do not absorb), for PMPS25 and PMPS1285, as a function of temperature.

The release of these temporary hindered monomers through some segmental chain rearrangements is much faster ($k_u = 1.21-1.55$ ns^{-1} at 20 °C) than the reciprocal decay time of the singlet state ($k_M = 0.27$ ns^{-1} at 20 °C), but it is one order of magnitude slower than the more common (local) relaxation at the dyad level ($k_a = 14.2-16.3$ ns^{-1} at 20 °C), and its activation energy contains an additional barrier about 3 kcal/mol (equal to the energy required to break one excimer-forming site).

The same results for rate constants and activation energies are found in different chain lengths. What varies systematically depending on chain length is the behavior at low temperatures.

On lowering the temperature, while the overall size of the chains contracts, the fraction of temporary hindered monomers first decreases (slightly) and then increases (more steeply). Finally, interchain aggregation sets on. The temperatures at which the increase in β and the aggregation start are higher the longer the chain.

References and Notes

(1) Salom, C.; Semlyen, J. A.; Clarson, S. J.; Hernández-Fuentes, I.; Maçanita, A. L.; Horta, A.; Piérola, I. F. *Macromolecules* **1991**, *24*, 6827.
(2) Maçanita, A. L.; Piérola, I. F.; Horta, A. *Macromolecules* **1991**, *24*, 1293.
(3) Goldenberg, M.; Emert, J.; Morawetz, H. *J. Am. Chem. Soc.* **1978**, *100*, 7171.
(4) Freire, J. J.; Piérola, I. F.; Horta, A. *Macromolecules* **1996**, *29*, 5143.
(5) Horta, A.; Piérola, I. F.; Rubio, A.; Freire, J. J. *Macromolecules* **1991**, *24*, 3121.
(6) Rubio, A.; Freire, J. J.; Piérola, I. F.; Horta, A. *Macromolecules* **1989**, *22*, 4014.
(7) Maçanita, A. L.; Horta, A.; Piérola, I. F. *Macromolecules* **1994**, *27*, 958.
(8) Vigil, M. R.; Renamayor, C. S.; Piérola, I. F.; Lima, J. C.; Melo, E. C.; Maçanita, A. L. *Chem. Phys. Lett.* **1998**, *287*, 379.
(9) Phillips, D.; Roberts, A. J.; Rumbles, G.; Soutar, I. *Macromolecules* **1983**, *16*, 1597.
(10) Itagaki, H.; Horie, K.; Mita, I. *Macromolecules* **1983**, *16*, 1395.
(11) Fredrickson, G. H.; Franck, C. W. *Macromolecules* **1983**, *16*, 572.
(12) Sienicki, K.; Durocher, G. *Macromolecules* **1991**, *24*, 1102.
(13) Webber, S. E. *Chem. Rev.* **1990**, *90*, 1469.
(14) Ng, D.; Yoshiki, K.; Guillet, J. E. *Macromolecules* **1983**, *16*, 568.
(15) Itagaki, H.; Obukata, N.; Okamoto, A.; Horie, K.; Mita, I. *J. Am. Chem. Soc.* **1982**, *104*, 4469.
(16) Ng, D.; Guillet, J. E. *Macromolecules* **1981**, *14*, 405.
(17) Nakahira, T.; Ishizuka, S.; Iwabuchi, S.; Kojima, K. *Macromolecules* **1982**, *15*, 1218.
(18) Maçanita, A. L. In *Plenary Lectures III Congreso de Fotoquímica*; Armesto, D., Orellana, G., Piérola, I. F., Eds.; UNED: Madrid, 1996; Chapter 4, pp 76−109.
(19) Lima, J. C. Ph.D. Thesis, IST, Lisboa, 1996; Chapter II, p 3.
(20) Holden, D. A.; Wang, P. Y. K.; Guillet, J. E. *Macromolecules* **1980**, *13*, 295.
(21) Torkelson, J. M.; Lipsky, S.; Tirrell, M. *Macromolecules* **1981**, *14*, 1601.
(22) Johnson, G. E.; Good, T. A. *Macromolecules* **1982**, *15*, 409.
(23) Gelles, R.; Frank, C. W. *Macromolecules* **1982**, *15*, 741.
(24) Zanocco, G.; Abuin, E.; Lissi, E.; Gargallo, L.; Radic, D. *Eur. Polym. J.* **1982**, *18*, 1037.
(25) Torkelson, J. M.; Lipsky, S.; Tirrell, M. *Macromolecules* **1983**, *16*, 326.
(26) Holden, D. A.; Kovarova, J.; Guillet, J. E.; Engel, D.; Rhein, T.; Schulz, R. C. *Eur. Polym. J.* **1984**, *20*, 105.
(27) Abuin, E.; Lissi, E.; Gargallo, L.; Radic, D. *Eur. Polym. J.* **1984**, *20*, 105.
(28) Major, M. D.; Torkelson, J. M. *Macromolecules* **1986**, *19*, 2801.
(29) Handa, T.; Utena, Y.; Yajima, H.; Katayama, R.; Ishii, T.; Yamauchi, T. *J. Phys. Chem.* **1986**, *90*, 6324.
(30) Utena, Y.; Yajima, H.; Ishii, T.; Handa, T. *Eur. Polym. J.* **1988**, *24*, 71.
(31) Tsai, F. J.; Torkelson, J. M. *Polymer* **1988**, *29*, 1004.
(32) Dias, F. B.; Lima, J. C.; Piérola, I. F.; Horta, A.; Maçanita, A. L. *J. Phys. Chem. A* **2001**, *105*, 10286.
(33) Dias, F. B.; Lima, J. C.; Maçanita, A. L.; Piérola, I. F.; Horta, A.; Maçanita, A. L. *J. Phys. Chem. A* **2000**, *104*, 17.
(34) Horta, A.; Piérola, I. F.; Maçanita, A. L. *Macromolecules* **2000**, *33*, 1213.
(35) Dias, F. B.; Lima, J. C.; Maçanita, A. L.; Clarson, S. J.; Piérola, I. F.; Horta, A. *Macromolecules* **2000**, *33*, 4772.
(36) Clarson, S. J.; Semlyen, J. A. *Polymer* **1986**, *27*, 1633.
(37) Maçanita, A. L.; Costa, F.; Costa, S.; Melo, E. C.; Santos, H. *J. Phys. Chem.* **1989**, *93*, 336.
(38) Striker, G. In *Deconvolution and Reconvolution of analytical Signals*; Bouchy, M., Ed.; DPIC: Nancy, 1982.
(39) Maçanita, A. L.; Danesh, P.; Peral, F.; Horta, A.; Piérola, I. F. *J. Phys. Chem.* **1994**, *98*, 6548.
(40) Ishii, T.; Handa, T.; Matsunaga, S. *Macromolecules* **1978**, *11*, 40.
(41) Salom, C.; Freire, J. J.; Hernández-Fuentes, I. *Polymer* **1989**, *30*, 615.

MA020402M